BMC Biotechnology

RESEARCH Open Access

Targeted cancer therapy potential of quercetin-conjugated with folic acid-modified nanocrystalline cellulose nanoparticles: a study on AGS and A2780 cell lines

Mozhgan Soltani[1*], Negar Ahmadzadeh[1], Hasti Nasiraei Haghighi[1], Niloufar Khatamian[1] and Masoud Homayouni Tabrizi[1*]

Abstract

This study investigates the effects of quercetin-conjugated nanocrystalline cellulose/cetyltrimethylammonium bromide/folic acid nanoparticles (NCC/CTAB/FA NPs) on AGS and A2780 cancer cell lines, focusing on their cytotoxicity and antioxidant capacity. Dynamic light scattering (DLS) analysis revealed an average particle size of 388.70 nm, suitable for cellular uptake and release kinetics. The NCC/CTAB/FA NPs exhibited a rod and spherical morphology and uniform distribution, as confirmed by field emission scanning electron microscopy (FESEM). Fourier-transform infrared (FTIR) spectroscopy confirmed the successful synthesis and functional group integration, supporting the NPs' ability for drug delivery. The encapsulation efficiency value was 81.17%, demonstrating the effective incorporation of Quercetin. Cytotoxicity assays indicated significant reductions in cell viability for AGS and A2780 cells with IC_{50} values of 3.2 µg/mL and 16.04 µg/mL, respectively, while HDF cells exhibited higher viability. Flow cytometry analysis revealed a dose-dependent induction of apoptosis in AGS cells, supported by changes in gene expression related to apoptosis and inflammation. Furthermore, antioxidant capacity assays demonstrated practical free radical scavenging abilities, with IC_{50} values of 151.65 µg/mL for ABTS and 349.54 µg/mL for DPPH. NCC/CTAB/FA/Quercetin NPs exhibit promising characteristics for targeted cancer therapy and antioxidant applications.

Keywords Quercetin, Nanoparticles, Cancer, Cytotoxicity, Antioxidant, Apoptosis

*Correspondence:
Mozhgan Soltani
soltani_m4@yahoo.com
Masoud Homayouni Tabrizi
mhomayouni6@gmail.com
[1]Department of Biology, Mashhad Branch, Islamic Azad University, Mashhad, Iran

Introduction

Cancer poses a significant medical challenge due to drug resistance in cancer cells, complicating effective disease management [1]. This challenge has prompted the exploration of novel therapeutic approaches that can overcome drug resistance and improve treatment outcomes [1–3]. Cancer drug resistance arises from various mutations in cancer cells. They can suppress tumor suppressor genes, inhibit apoptosis, activate resistance mechanisms, and weaken the immune system [4, 5]. For instance, in human ovarian cancer cell line A2780, mutations in the TP53 gene can hinder apoptosis [6], while alterations in the BRCA1 and BRCA2 genes impact DNA repair mechanisms [7]. Changes in the EGFR gene can enhance cell proliferation [8], and mutations in the KRAS gene may contribute to resistance by activating signaling pathways that promote cell survival, even in drug treatment [9]. Also, mutations in TP53, PIK3CA, CDKN2A, and HER2 in gastric adenocarcinoma cell line AGS cells contribute to drug resistance by disrupting apoptosis, enhancing survival signaling, and promoting cell proliferation [10]. These findings highlight the critical need for innovative strategies to target these mechanisms and improve cancer treatment effectiveness [11, 12]. Recent interest in natural compounds for cancer therapy has highlighted Quercetin, a polyphenolic flavonoid found in many fruits and vegetables [13]. Quercetin exhibits antioxidant, anti-inflammatory, antiviral, and anticancer properties [14–16]. It shows potential in modulating pathways related to apoptosis and autophagy, making it a strong candidate for overcoming drug resistance in cancer cells [17, 18]. Studies suggest Quercetin can promote apoptosis and other cell death forms by influencing reactive oxygen species (ROS) metabolism [19]. This may sensitize cancer cells to conventional therapies and overcome drug resistance. Quercetin also enhances immune function and regulates tumor suppressor gene activity, indicating its potential as an anticancer agent [20]. However, its low water solubility, chemical instability, and poor bioavailability limit its clinical application and effective therapeutic doses [21]. In light of these attributes, implementing drug delivery systems (DDSs) to target this compound for transport to cancerous tissues effectively addresses the limitations of quercetin therapy [22]. DDSs such as NPs and liposomes play a crucial role in cancer treatment, enabling targeted and controlled release of therapeutic agents to tumor sites [11, 23]. They enhance the bioavailability of anticancer drugs, improve solubility, and minimize systemic toxicity by limiting exposure to healthy tissues [24]. Through active targeting with cancer-specific ligands, DDSs increase tumor drug accumulation and reduce side effects [25].

Among various DDSs, nanocrystalline cellulose/cetyltrimethylammonium bromide/folic acid nanoparticles (NCC/CTAB/FA NPs) are a promising vehicle for delivering therapeutic agents specifically to cancer cells due to their unique characteristics [26, 27]. NCC is a biopolymer known for its high surface area, biodegradability, and biocompatibility. It can be an effective nanocarrier for drug delivery, enabling better dispersion of hydrophobic compounds like Quercetin [28, 29]. When combined with CTAB, a surfactant that improves the solubility of poorly soluble compounds, the formulation's effectiveness can be further enhanced. CTAB also increases the stability of the nanocarrier and facilitates sustained release of the encapsulated agent [30]. Additionally, the incorporation of FA into this system improves targeting capabilities. FA is recognized for its high affinity for folate receptors, often overexpressed in various cancer cell types, including ovarian and gastric cancer. By leveraging the FA moiety, this nanocarrier system can enhance the selective accumulation of Quercetin at tumor sites, minimizing systemic toxicity and improving therapeutic efficacy [31]. This innovative approach holds significant potential for targeted delivery and enhanced bioavailability of Quercetin, thereby maximizing its anticancer effects.

In this context, the present study aimed to evaluate the impacts of quercetin-conjugated with NCC/CTAB/FA NPs on the A2780 and the AGS in an in vitro setting. A2780 cells represent a more chemosensitive ovarian cancer model, while AGS cells are known for their aggressive nature and resistance to conventional treatments. They represent distinct responses to chemotherapy, providing a broader understanding of Quercetin's efficacy across different cancer types. By elucidating the impact of this novel formulation on cancer cell viability and apoptosis, this study seeks to contribute valuable insights into the potential of quercetin-based therapies for overcoming drug resistance in cancer. We introduce a unique NCC/CTAB/FA/Quercetin NPs formulation that demonstrates selective cytotoxicity towards AGS and A2780 cancer cell lines, effective pH-dependent drug release, and significant antioxidant properties, highlighting their potential as innovative therapeutic agents in cancer therapy.

Materials and methods

Fabrication of NCC/CTAB/FA NPs

This study prepared NCC from microcrystalline cellulose (MCC) using sulfuric acid treatment. For this purpose, 10 g of MCC (Merck) was mixed with 64% sulfuric acid (Merck) and incubated at 60 °C for 90 min, with continuous stirring. The reaction was stopped by adding 800 mL of cold distilled water, followed by centrifugation and multiple washings. The resulting suspension was dialyzed for 7 days and ultrasonically dispersed to obtain a homogeneous white suspension, which was subsequently lyophilized. To functionalize the NCC with

CTAB (Sigma-Aldrich), 200 mg of NCC was added to an aqueous solution containing 4 μM of CTAB, and the mixture was stirred at 60 °C for 3 h to ensure complete functionalization. The mixture was then centrifuged to remove excess CTAB. Quercetin (Sigma-Aldrich) was incorporated into the NCC-CTAB NPs by initially dissolving Quercetin in deionized distilled water and ethanol to form a concentrated solution (10 mg/ 2mL). This solution was then gradually added to the NCC-CTAB solution while stirring to ensure an even distribution of Quercetin. This mixture was subsequently centrifuged and lyophilized. For the final step of functionalization with FA, FA (Thermo Scientific) was first activated using N-hydroxysuccinimide (NHS) (Sigma-Aldrich) and 1-ethyl-3-(3-dimethylaminopropyl) carbodiimide (EDC) (Sigma-Aldrich). The activated FA solution was then added to the NCC-CTAB-quercetin solution and incubated on a stirrer at room temperature for 24 h, followed by centrifugation and lyophilization.

Characterization of NCC/CTAB/FA/Quercetin NPs

The hydrodynamic size and distribution of the particles in aqueous solution were characterized using dynamic light scattering (DLS) (Nicomp N3000 Nanoparticle Size Analyzer; Entegris), as detailed in reference [32]. This method allows for assessing the particle size distribution and stability in suspension. Additionally, we utilized field emission scanning electron microscopy (FESEM) (SU5000; Hitachi) to examine the particle morphology, while Fourier transform infrared spectroscopy (FTIR) (Tensor II; Bruker) analysis was conducted to investigate the functional groups.

Cell culture

The AGS (F-1053013c) and A2780 (F-1036013) human cancer cell lines, along with human dermal fibroblast (HDF) cells (F-1049024), were obtained from the Ferdowsi University of Mashhad, Iran. AGS cells, a gastric cancer cell line, were cultured in Roswell Park Memorial Institute (RPMI)-1640 medium (Gibco) supplemented with 10% fetal bovine serum (FBS) (Gibco) and 1% penicillin-streptomycin. A2780 cells, an ovarian cancer cell line, were maintained in DMEM (Gibco) with 10% FBS and 1% penicillin-streptomycin. HDF cells were cultured in DMEM (Gibco) with 10% FBS and 1% penicillin-streptomycin. All cell lines were incubated at 37 °C in a humidified atmosphere with 5% CO2. Cells were passaged when they reached 80% confluence using a 0.25% trypsin-EDTA solution. Cell viability was assessed using the trypan blue exclusion assay, ensuring that only cultures with more than 95% viability were used for subsequent experiments. The NPs were dissolved in the respective cell culture medium and administered to passage 3 cells at the specified concentrations for treatments.

Cytotoxicity assay

The cytotoxic effects of NCC/CTAB/FA/Quercetin NPs on AGS and A2780 cancer cell lines (passage 3), as well as on HDF cells, were evaluated using the MTT assay, a widely used method for assessing cell viability based on mitochondrial activity. The cells were seeded at 5×10^3 in 96-well plates for 24 h. Subsequently, the cells were exposed to NCC/CTAB/FA/Quercetin NPs at 0.93, 1.8, 3.75, 7.5, 15, 30, and 60 μg/mL concentrations. Following a 48-h incubation, 20 μl of MTT reagent (5 mg/mL) was added to each well, and the plates were incubated in the dark at 37 °C for 4 h. Following the removal of the medium, 200 μl of dimethyl sulfoxide (DMSO; Sigma) was introduced to facilitate the dissolution of the formazan crystals for one hour. Subsequently, the absorbance at 570 nm was measured using a microplate reader. Cell viability was expressed as a percentage relative to the control group.

Annexin V-FITC/PI assay

The Annexin V-FITC apoptosis staining detection kit (Abcam, ab14085) assessed apoptosis according to the manufacturer's instructions. Following a 48-h exposure of AGS cells to NCC/CTAB/FA/Quercetin NPs at 1, 3, and 30 μg/mL concentrations, the cells were trypsinized and centrifuged. Subsequently, 1×10^5 cells were suspended in 500 μl of binding buffer (1X) and incubated with 5 μl of annexin V-FITC and 5 μl of propidium iodide (PI) at 25 °C for 5 min in the dark. The cell suspension was centrifuged, and the cell pellet was resuspended in 400 μl of binding buffer. Finally, the cell suspension was analyzed using flow cytometry to determine the percentage of early apoptotic cells (Annexin V+, PI-), late apoptotic cells (Annexin V+, PI+), and necrotic cells (Annexin V-, PI+). It must be noted that the 3 μg/mL concentration corresponds to the IC_{50} concentration, while the other two doses were chosen to induce cell death at around 25% and 75%, respectively.

Acridine orange/propidium iodide (AO/PI) staining

AGS cells were seeded at a density of 1×10^4 cells per well in 6-well plates and incubated for 24 h. The cells were treated with NCC/CTAB/FA/Quercetin NPs for 48 h. After treatment, the cells were trypsinized and washed with phosphate-buffered saline (PBS). The cells were resuspended in a PBS solution containing acridine orange (AO) at 1 μg/mL concentration and propidium iodide (PI) at 5 μg/mL and incubated at room temperature for 10 min. Finally, the cells were washed and examined under a fluorescence microscope (Carl Zeiss, Jena, Germany).

Real-time polymerase chain reaction (Real time-PCR)

The mRNA expression of caspase 8, tumor necrosis factor (TNF), superoxide dismutase (SOD), and NF-κB was evaluated using real-time polymerase chain reaction (PCR). Briefly, RNA extraction from AGS cells was performed using a QIAGEN total RNA extraction kit, and the extracted RNA was quantified and qualified by a ThermoFisher Nanodrop ND-1000 spectrophotometer at 260 nm. The isolated mRNA was then transcribed into complementary DNA (cDNA) using Moloney Murine Leukemia Virus Reverse Transcriptase (M-MLV RT; Promega). Subsequently, real-time PCR was conducted using a Corbett thermal cycler, specific primers (see Table 1), and Bio-Rad SYBR Green Master Mix. The comparative Ct (cycle threshold) method was employed to normalize gene expression levels, utilizing glyceraldehyde-3-phosphate dehydrogenase (GAPDH) as a reference. The mean Ct values from triplicates were used to calculate the expression level of the target gene via the $2^{-\Delta\Delta Ct}$ formula.

Antioxidant activity assay

The antioxidant capacity of NCC/CTAB/FA/Quercetin NPs was evaluated by neutralizing ABTS and DPPH free radicals. Glutathione was used as a control. In the ABTS assay, a stock solution was prepared by combining equal volumes of 7 mM ABTS and 2.45 mM potassium persulfate, which was then incubated in the dark at 25 °C for 12 h. Subsequently, the solution was diluted with ethanol to an absorbance of 0.70 at 734 nm. A series of NCC/CTAB/FA/Quercetin NP concentrations were introduced to the diluted ABTS solution in a 96-well plate, and the absorbance was subsequently measured after 6 min. For the DPPH assay, a 0.1 mM DPPH solution was prepared in methanol and incubated for 30 min in a dark place. Subsequently, different concentrations of NCC/CTAB/FA/Quercetin NPs were introduced, and the absorbance was measured at 517 nm. The radical scavenging activity for both ABTS and DPPH assays was determined using the following formula: The percentage inhibition was calculated as (%): (control absorbance – sample absorbance) / control absorbance × 100.

Table 1 Specific primer sequences for real-time PCR

Primer	Sequence
Caspase 8	F: 5′- GAAAAGCAAACCTCGGGGATAC – 3′ R: 5′- CCAAGTGTGTTCCATTCCTGTC – 3′
TNF	F 5′- CAGAGGGAAGAGTTCCCCAG – 3′ R 5′- CCTTGGTCTGGTAGGAGACG – 3′
NF-κB	F 5′- CCTGCTTCTGGAGGGTGATG – 3′ R 5′- GCCGCTATATGCAGAGGTGT – 3′
SOD	F 5′- CAGCATGGGTTCCACGTCCA – 3′ R 5′- CACATTGGCCACACCGTCCT – 3′
GAPDH	F 5′- GCAGGGGGGAGCCAAAAGGGT – 3′ R 5′- TGGGTGCCAGTGATGGCATGG – 3′

Statistical analysis

Statistical analysis was performed using SPSS software. The normality of the data was evaluated using the Shapiro-Wilk test. A one-way analysis of variance (ANOVA) was conducted for comparisons among multiple groups. Subsequent comparisons were conducted using Tukey's test to identify specific group differences. A p-value of less than 0.05 was deemed to indicate statistical significance. All data are presented as means ± standard deviations (SD).

Results

This study aimed to assess the effects of quercetin-conjugated NCC/CTAB/FA NPs on AGS and A2780 cancer cell lines, explicitly evaluating their cytotoxicity and antioxidant capacity.

DLS assay

The DLS analysis of the NCC/CTAB/FA/Quercetin nanoparticles (NPs) (Fig. 1A) reveals a Z-average particle size of 354.4 ± 65.37 nm, which falls within the generally accepted range for nanocarriers (1–1000 nm). The Polydispersity index (PDI) of 0.33 ± 0.14 suggests a moderately narrow size distribution, indicating that most particles are uniformly sized. Additionally, the mean number diameter of 181.17 ± 75.4 nm suggests that a significant proportion of the NPs are below 300 nm. Lastly, the negative zeta potential of -27.05 ± 1.64 mV indicates appropriate colloidal stability. All data are averages from three repeated measurements.

FESEM

The FESEM micrograph (Fig. 1B) of the NCC/CTAB/FA/Quercetin NPs visualizes their morphology and structure at the nanoscale. The image reveals that the NPs predominantly have a rod and spherical shape. The particles are uniformly dispersed and show no signs of aggregation. The surface texture of the NPs exhibits some roughness, which may enhance interactions with biological membranes and potentially improve drug release profiles. A scale bar in the image indicates a measurement of 200 nm, confirming that the observed features fall within the nanometer range, consistent with the intended design of the nanocarrier system.

FTIR spectroscopy

As shown in Fig. 2A, the FTIR spectroscopy of Quercetin revealed a complex spectrum with several characteristic peaks linked to its functional groups. The broad bands around 3423.84 cm^{-1} and 3378.89 cm^{-1} indicate hydroxyl (-OH) groups, contributing to its antioxidant properties. The peak at 1672.07 cm^{-1} suggests carbonyl (C = O) stretching from a ketone, while those near 1616.50 cm^{-1} indicate conjugated double bonds in the aromatic rings.

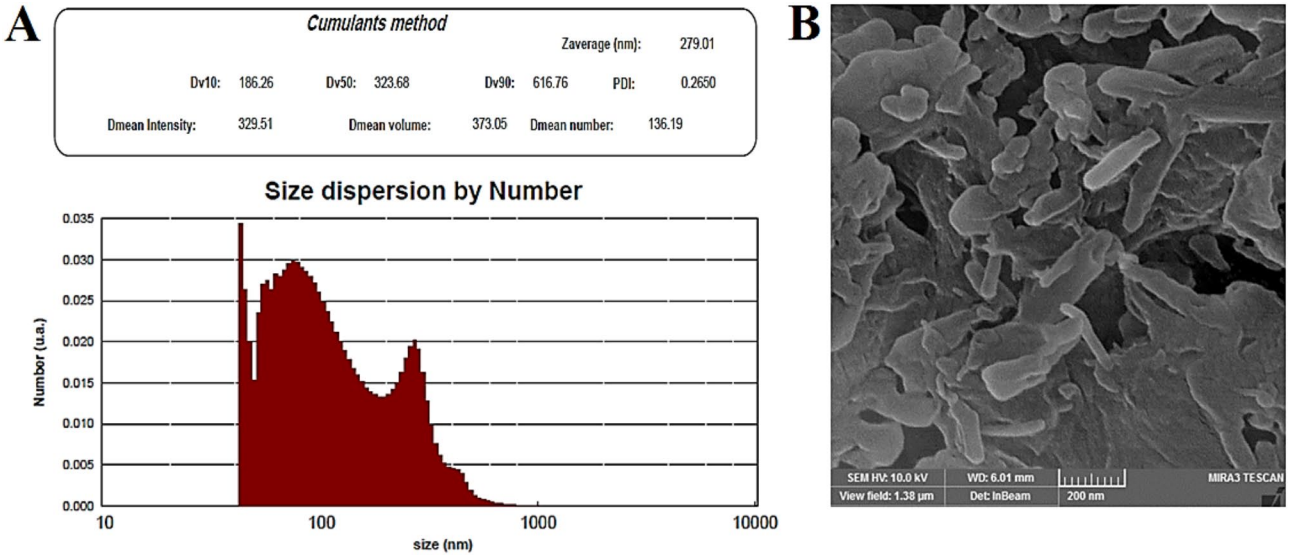

Fig. 1 (**A**) The DLS assay for NCC/CTAB/FA/Quercetin NPs reveals a Z-average particle size of 354.4 ± 65.37 nm, a polydispersity index of 0.33 ± 0.14, and a zeta potential of -27.05 ± 1.64 mV. All data are averages from three repeated measurements. (**B**) The field emission scanning electron microscopy (FESEM) micrograph of NCC/CTAB/FA/Quercetin NPs reveals their rod and spherical shape, uniform dispersion, and surface texture. With a size scale of 200 nm, these characteristics suggest successful fabrication and potential effectiveness in targeted drug delivery and cancer therapy

Peaks at 1513.13 cm^{-1} and 1457.52 cm^{-1} are related to C = C stretching typical of aromatic compounds. Peaks at 1244.33 cm^{-1} and 1165.63 cm^{-1} correspond to C-O bond stretching, indicating methoxy or hydroxyl groups. Lower frequency peaks, such as 706.18 cm^{-1} and 597.87 cm^{-1}, reflect out-of-plane bending vibrations.

Additionally, the FTIR spectrum of the NCC/CTAB/FA/Quercetin NPs (Fig. 2B) shows a broad peak at 3385.33 cm^{-1}, indicating hydroxyl (-OH) groups from cellulose and FA, contributing to hydrophilicity. Peaks at 2915.09 cm^{-1} and 2847.67 cm^{-1} correspond to C-H stretching from the alkyl groups in CTAB, suggesting effective surfactant encapsulation. Absorption bands at 1648.29 cm^{-1} and 1605.45 cm^{-1} indicate C = O stretching from the carbonyl groups of Quercetin and FA, while peaks at 1436.33 cm^{-1} and 1409.31 cm^{-1} correspond to both aromatic and aliphatic C-H bending, emphasizing the hybrid nature of the composite matrix. Lower wavenumber peaks around 1162.22 cm^{-1} and 1115.10 cm^{-1} can be attributed to C-O stretching from cellulose and FA.

Encapsulation efficacy and drug release profile

Encapsulation efficiency was evaluated using the spectrophotometric method at 375 nm wavelength (Fig. 3A). The measured 81.17% encapsulation efficiency indicates the successful incorporation of a significant amount of Quercetin into the NCC/CTAB/FA NPs. In addition, Fig. 3B illustrates the cumulative release profile of Quercetin at two different pH levels: 5.5 and 7.4. At the lower pH of 5.5, the release of Quercetin gradually increases over time, reaching 87.9% after 72 h. In contrast, at the higher pH of 7.4, the release is significantly slower, with the cumulative release only reaching approximately 39.3% after the same 72 h.

Cytotoxicity assay

Figure 4 presents data on the cytotoxic effects of NCC/CTAB/FA/Quercetin NPs on various cancer cell lines, including A2780 and AGS and HDF cells as a control group. The results indicate that as the concentration of the NPs increases from 0 to 60 µg/mL, cell viability is significantly decreased for both the A2780 (Fig. 3A) and AGS (Fig. 3B) cells ($P < 0.001$). In contrast, HDF cells maintain relatively higher viability across the tested concentrations, showing a notable decline only at 15, 30, and 60 µg/mL (Fig. 3B; $P < 0.001$). The IC50 values for the A2780, AGS, and HDF cell lines were determined to be 16.04 µg/mL, 3.2 µg/mL, and 50.21 µg/mL, respectively, indicating a differential response between cancerous and normal cells.

Annexin V-FITC/PI assay

The flow cytometry analysis of apoptosis in AGS cells stained with Annexin V-FITC and PI demonstrated significant apoptotic activity in a dose-dependent manner following treatment with NCC/CTAB/FA/Quercetin NPs at concentrations of 1, 3, and 30 µg/mL (Fig. 5). In the control group, the percentages of early and late apoptotic cells were minimal, at 2.93% and 2.27%, respectively. At the lowest 1 µg/mL concentration, early and late apoptotic cell percentages increased to 9.52% and 13.2%, respectively, indicating significant apoptosis induction. As the concentration rose to 3 µg/ml, the early and late apoptotic cell percentages increased to 18.3% and 26.3%,

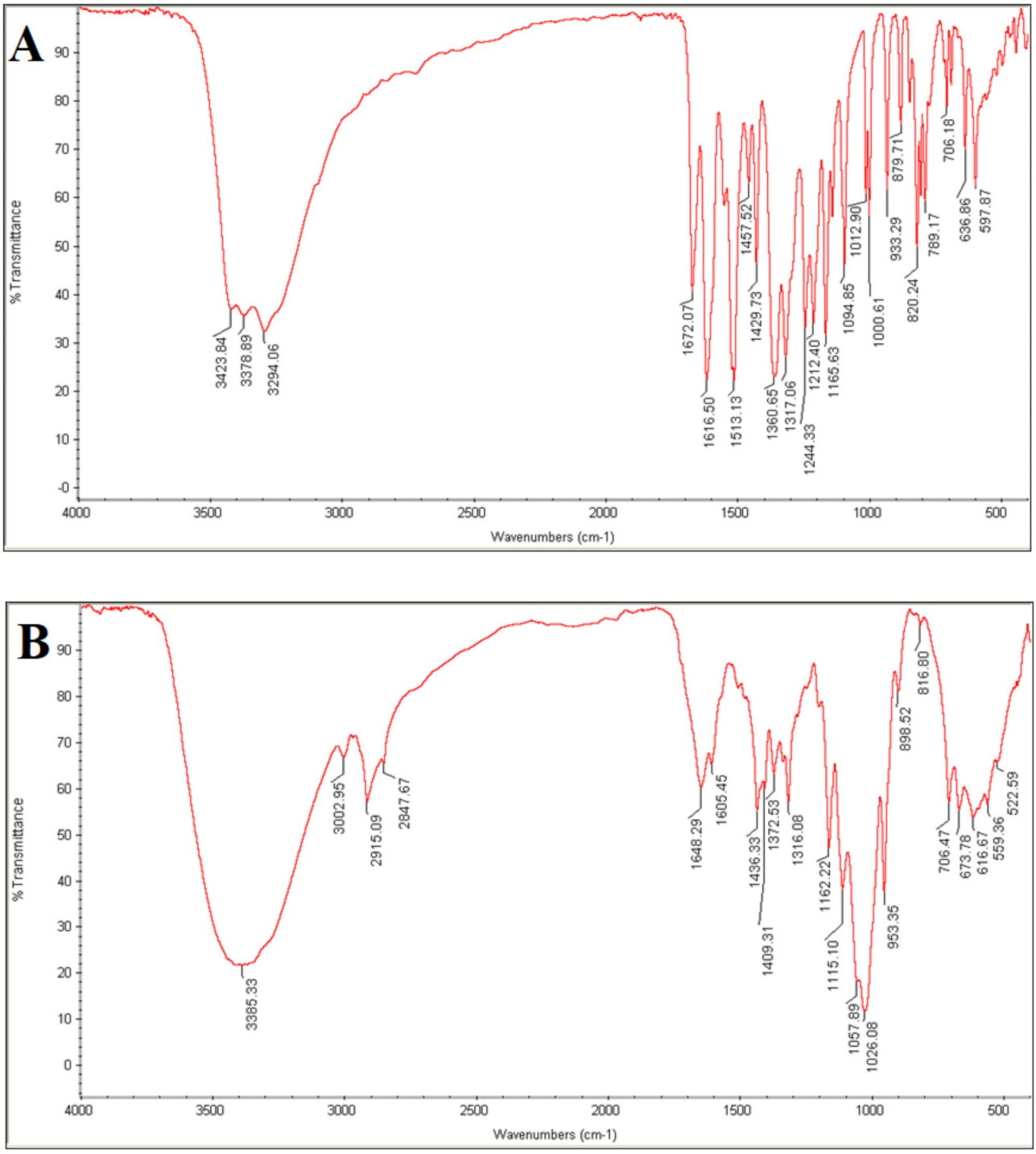

Fig. 2 FTIR spectroscopy. (**A**) The FTIR spectrum of Quercetin highlights key functional groups, including -OH, C = O, and C = C bonds. (**B**) The FTIR spectrum of NCC/CTAB/FA/Quercetin NPs shows OH, C-H, and C = O stretches, confirming successful NP synthesis

respectively. At the highest concentration of 30 µg/mL, the apoptotic populations became even more pronounced, with 14.8% of cells in early apoptosis and 40.9% in late apoptosis.

AO/PI staining

The AO/PI staining of AGS cells treated with varying concentrations of NCC/CTAB/FA/Quercetin NPs reveals distinct patterns based on treatment concentration (Fig. 6). In untreated controls, the cells exhibit uniform green fluorescence, indicating a healthy population.

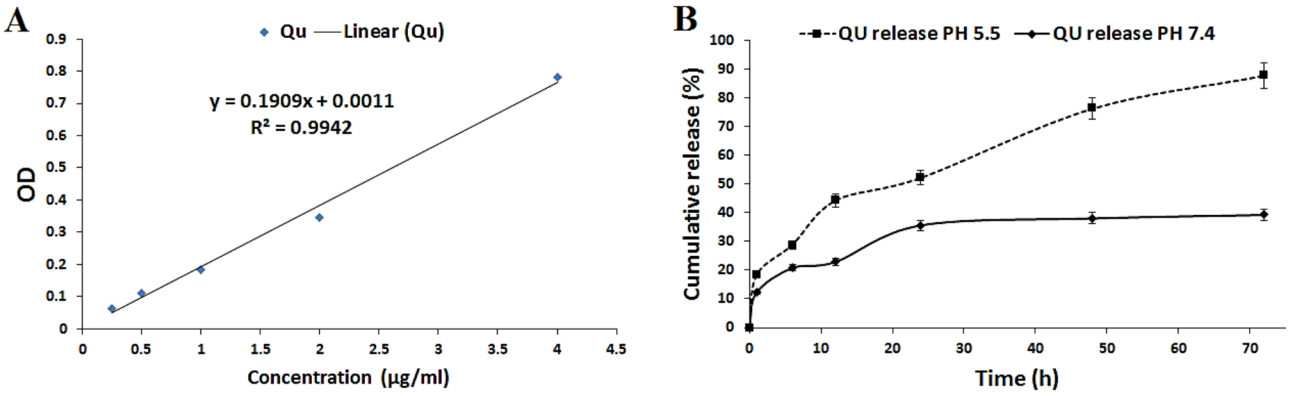

Fig. 3 Quercetin Encapsulation and pH-Dependent Release Profile. (**A**) The image shows the encapsulation efficiency and cumulative release behavior of the drug Quercetin. The encapsulation efficiency, measured using spectrophotometry, was 81.17%, indicating the successful incorporation of a significant amount of Quercetin into the NP formulation. (**B**) The cumulative release profile demonstrates that Quercetin exhibits pH-dependent release, with faster release at the lower pH of 5.5 compared to the higher pH of 7.4. This suggests that Quercetin's solubility and dissolution are enhanced in acidic environments, which could impact its absorption and bioavailability

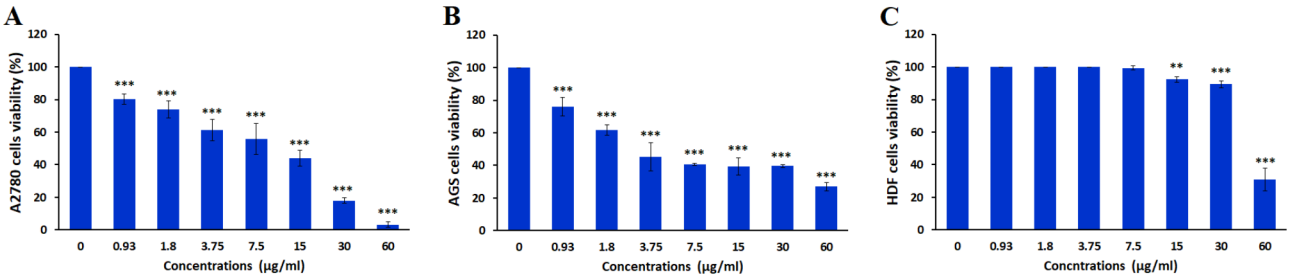

Fig. 4 Cytotoxic effects of NCC/CTAB/FA/Quercetin NPs on cancer cell lines. NPs significantly reduce cell viability in a concentration-dependent manner, as observed in A2780 (**A**) and AGS (**B**). In contrast, HDF cells (**C**) show reduced viability only at higher concentrations. The IC_{50} values are 16.04 µg/mL for A2780, 3.2 µg/mL for AGS, and 50.21 µg/mL for HDF, indicating that cancer cells are selectively targeted. The data is presented as mean ± standard deviation (SD), and statistical significance is denoted as ** $P < 0.01$ and *** $P < 0.001$

At a lower concentration of 1 µg/mL, some cells show a combination of green and orange/red fluorescence, suggesting the presence of both viable and apoptotic cells. When the concentration is increased to 3 µg/mL, there is a noticeable increase in cells with orange/red fluorescence, which signifies late apoptotic or necrotic cells and reflects a higher level of cell death. At the highest concentration of 30 µg/mL, most cells display strong orange/red fluorescence, indicating a significant induction of apoptosis and cell death. In contrast, the green fluorescence—representing viable cells—substantially decreases.

Gene expression assay

Figure 7 illustrates the mRNA expression levels of caspase 8, TNF, SOD, and NF-κB in AGS cancer cells treated with various concentrations of NCC/CTAB/FA/Quercetin NPs. Caspase 8 expression significantly increased at 30 µg/mL, suggesting that higher concentrations may enhance apoptotic signaling. This could benefit cancer therapy by promoting cell death in malignant cells. In contrast, TNF expression is significantly reduced at concentrations of 3 and 30 µg/mL, indicating that the treatment may exert an anti-inflammatory effect. This effect could help mitigate the inflammatory microenvironment often associated with cancer progression. Moreover, NF-κB expression significantly decreases at 30 µg/mL, suggesting that a high concentration of NPs may inhibit this key transcription factor involved in inflammatory responses, potentially reducing tumorigenesis. On the other hand, SOD expression is significantly low at 1 µg/mL and 3 µg/mL, indicating a potential impairment in antioxidant defenses at these concentrations. However, 30 µg/mL recovery suggests a dose-dependent response that may enhance antioxidant capacity at higher concentrations.

Antioxidant capacity assay

The antioxidant capacity of NCC/CTAB/FA/Quercetin NPs was evaluated by measuring their ability to inhibit ABTS and DPPH free radicals, as shown in Fig. 8A. The ABTS radical scavenging activity steadily increases to 500 µg/mL, reaching approximately 97.23% inhibition. The DPPH radical scavenging activity also increases with concentration but at a slower rate compared to

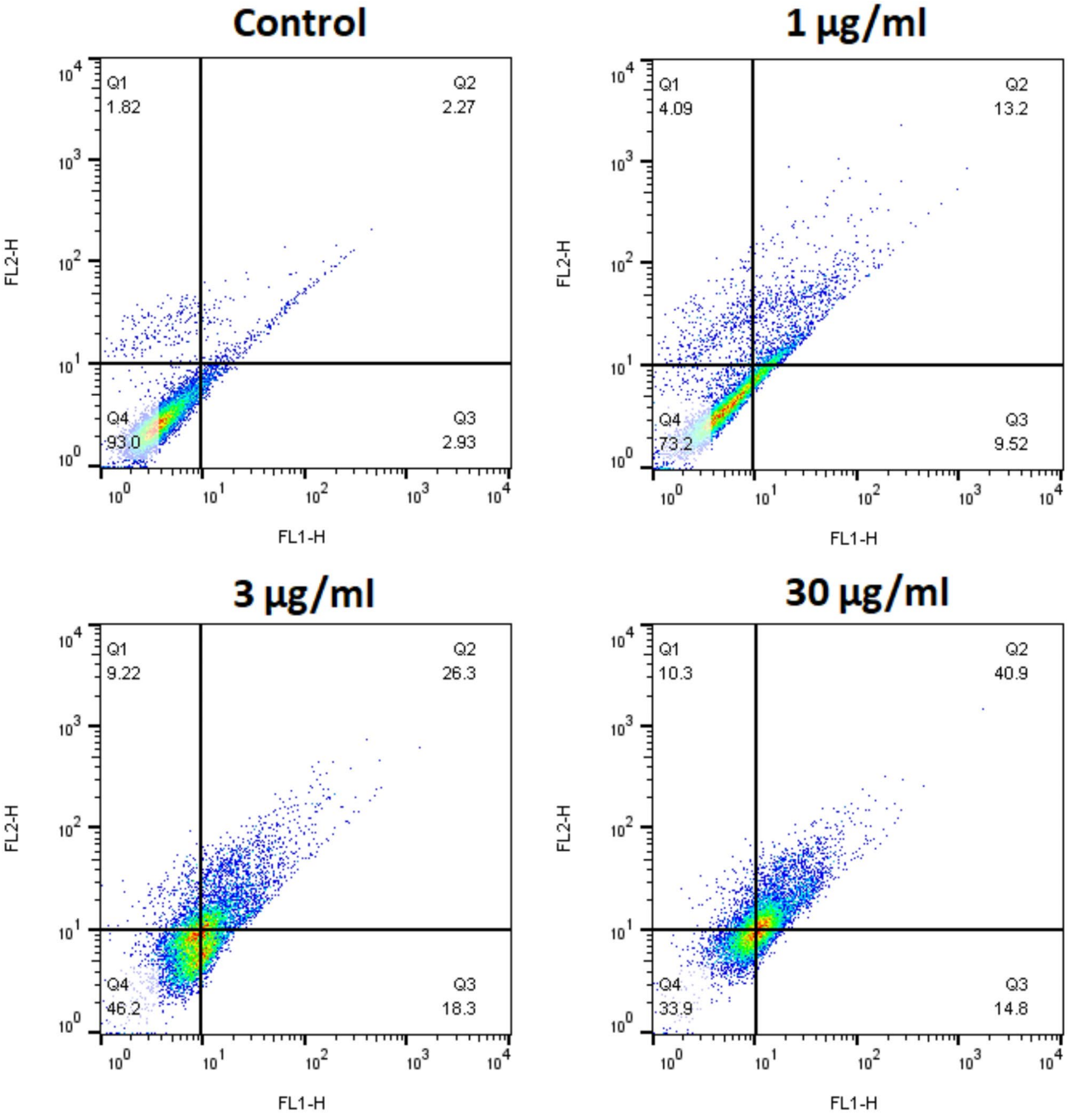

Fig. 5 Flow cytometry analysis of apoptosis in AGS cells treated with NCC/CTAB/FA/Quercetin NPs. Control cells showed minimal early (2.93%) and late (2.27%) apoptotic rates. At 1 µg/mL, early and late apoptosis increased to 9.52% and 13.2%. At 3 µg/mL, these rose to 18.3% and 26.3%, and at 30 µg/mL, 14.8% were in early apoptosis and 40.9% in late apoptosis, indicating dose-dependent apoptosis induction

ABTS. At higher concentrations (above 1000 µg/mL), both ABTS and DPPH inhibition levels reach 100%. The NCC/CTAB/FA/Quercetin NPs exhibited IC_{50} values of 151.65 µg/mL for ABTS inhibition and 349.54 µg/mL for DPPH inhibition. Glutathione exhibits a similar pattern, with ABTS inhibition reaching 100% at higher concentrations, while DPPH inhibition plateaus around 97.28% (Fig. 8B).

Discussion

The rising cancer mortality rate highlights the urgent need to advance cancer treatments through ongoing research [33, 34]. Current cancer drug therapies are effective but face challenges with tumor specificity, adverse effects, and resistance potential [35, 36]. In recent years, there has been a promising shift towards targeted therapy, which aims to eliminate cancer cells

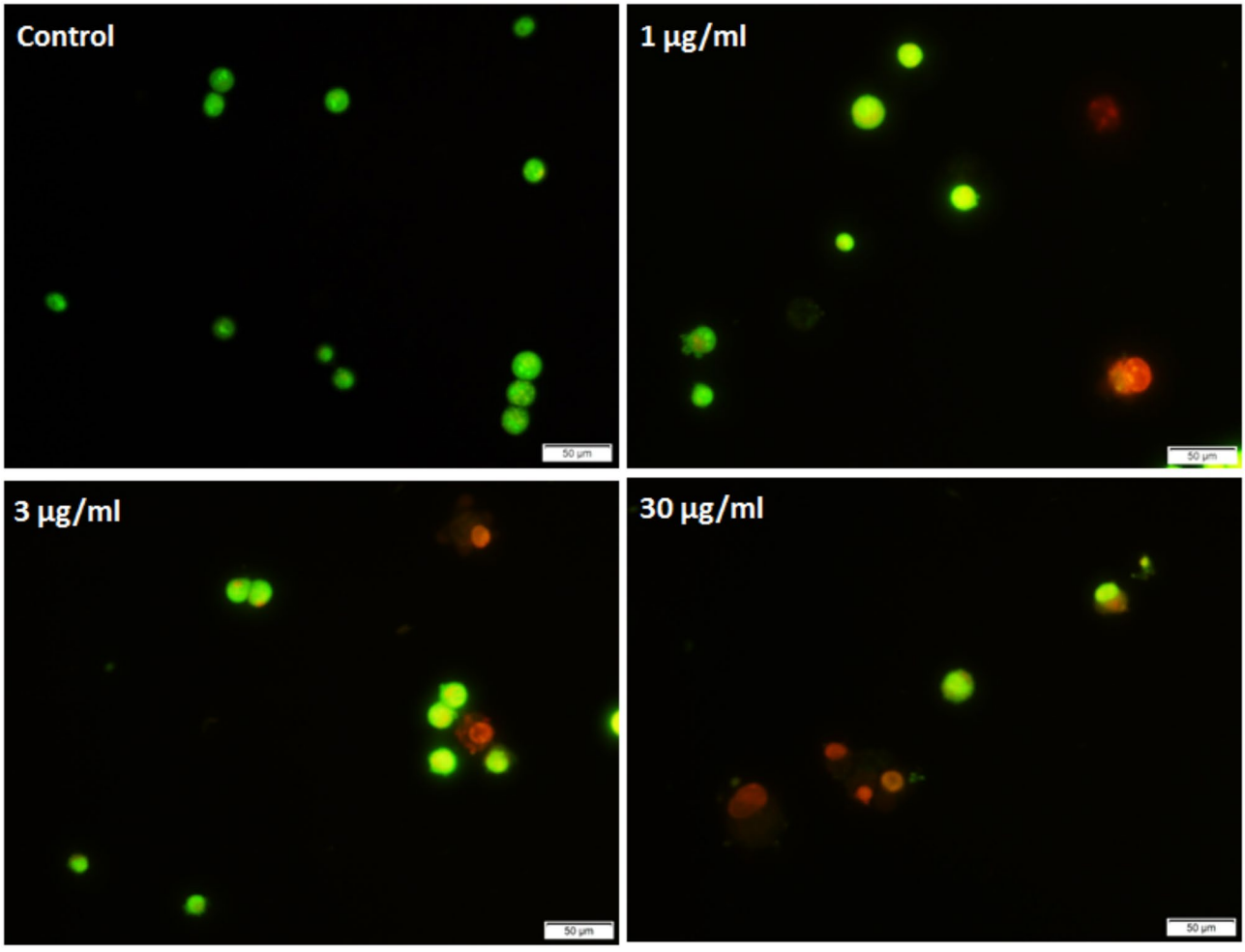

Fig. 6 AO/PI staining of AGS cells treated with NCC/CTAB/FA/Quercetin NPs shows concentration-dependent effects. Untreated controls show healthy green fluorescence. At 1 µg/mL, some cells display green and orange/red fluorescence, indicating viability and early apoptosis. At 3 µg/mL, increased orange/red fluorescence suggests late apoptosis or necrosis. At 30 µg/mL, strong orange/red fluorescence indicates significant apoptosis and cell death, demonstrating the therapeutic potential of these NPs for gastric cancer

while minimizing the impact on normal cells [37]. NPs have emerged as groundbreaking DDSs in cancer therapy, offering improved targeting and reduced systemic toxicity compared to traditional treatments [38]. Their unique properties, such as small size, enable passive targeting through enhanced permeability and retention (EPR), allowing NPs to accumulate in tumor tissues while sparing healthy cells [39]. This targeted approach enhances the pharmacokinetics of chemotherapeutic agents and addresses challenges such as multidrug resistance by modifying drug release mechanisms and overcoming barriers created by the tumor microenvironment [40]. For example, smart NPs can be designed to respond to specific biological stimuli, releasing their therapeutic payload precisely at the tumor site [41]. This maximizes efficacy while minimizing side effects. However, despite these advancements, several challenges remain, including the need for extensive clinical validation, potential immunological reactions, and issues related to scaling production for widespread clinical use. The future of this field depends on ongoing research into novel NP formulations and combinations that could further enhance their therapeutic index and clinical applicability in oncology.

On the other hand, although Quercetin shows potential as an anticancer agent, its clinical use is hindered by poor bioavailability and rapid metabolism. While nanocarrier-based DDSs improve tumor delivery, challenges like off-target effects, toxicity of carrier materials, and complex interactions with the tumor microenvironment remain. Addressing these issues will require more research to optimize Quercetin formulations and DDS designs for safe and effective cancer treatment. In this context, the current study explored the effects of NCC/CTAB/FA/Quercetin NPs on AGS and A2780 cancer cell lines, focusing on their cytotoxicity and antioxidant capacity.

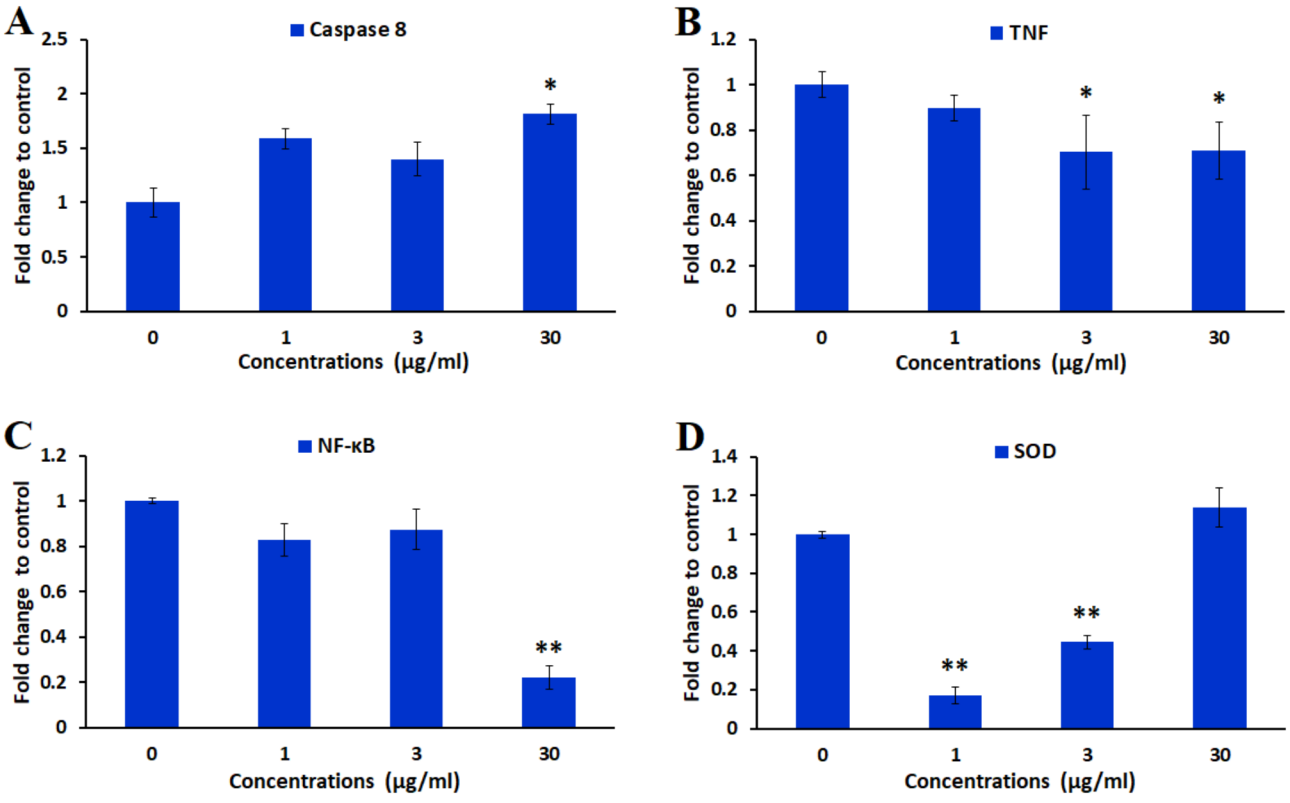

Fig. 7 Real-time PCR assay for mRNA expression levels of caspase 8, TNF, SOD, and NF-κB in AGS cells treated with different concentrations of NCC/CTAB/FA/Quercetin NPs. (**A**) Caspase 8 expression significantly increases at 30 µg/mL in the cells treated with NCC/CTAB/FA/Quercetin NPs, indicating enhanced apoptosis. (**B**) TNF and (**C**) NF-κB expressions decrease at 3 and 30 µg/mL, suggesting anti-inflammatory effects and potentially reducing tumorigenesis. (**D**) SOD shows low expression at 1 and 3 µg/mL but recovers at 30 µg/mL, indicating a dose-dependent enhancement of antioxidant capacity. The data is presented as mean ± standard deviation (SD), and statistical significance is denoted as * $P < 0.05$ and ** $P < 0.01$

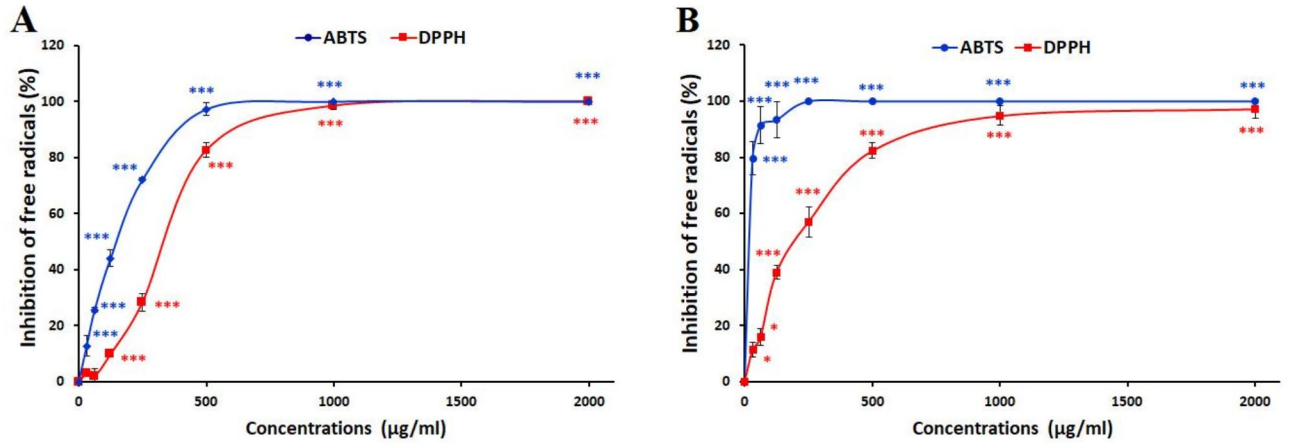

Fig. 8 Antioxidant assay. (**A**) The antioxidant capacity of NCC/CTAB/FA/Quercetin NPs was evaluated using ABTS and DPPH assays. ABTS inhibition reached about 97.23% at 500 µg/mL, while DPPH inhibition plateaued at 100% above 1000 µg/mL. IC50 values were 151.65 µg/mL for ABTS and 349.54 µg/mL for DPPH. (**B**) Glutathione achieved 100% ABTS inhibition and a DPPH plateau at 97.28%. These findings highlight the antioxidant properties of NCC/CTAB/FA/Quercetin NPs. The data is presented as mean ± standard deviation (SD), and statistical significance is denoted as * $P < 0.05$ and *** $P < 0.001$

The study's results demonstrate the successful synthesis and characterization of quercetin-conjugated NCC/CTAB/FA NPs, highlighting their potential for targeted drug delivery and cancer therapy. DLS analysis revealed appropriate particle size and distribution. Our NCC/CTAB/FA/Quercetin formulation has a mean NP size of 268.30 nm and a Z-average size of 388.70 ± 19.43 nm, ideal for effective drug delivery (1–1000 nm). This size

range facilitates cellular uptake through endocytosis and allows NPs to accumulate in tumor tissues due to the enhanced EPR effect. With a significant proportion below 200 nm and a negative zeta potential of -28.1 ± 11.64 mV, our formulation demonstrates good colloidal stability and prevents aggregation. Including CTAB, FA, and Quercetin may enhance drug release kinetics by increasing the surface area for diffusion, confirming the design's suitability for targeted cancer therapy. FESEM provided visual evidence of the rod and spherical morphology and uniform distribution of the NPs, both crucial for enhanced cellular uptake and consistent drug delivery. The rough surface texture may improve interactions with biological membranes, potentially enhancing drug release profiles. FTIR spectroscopy also confirmed the successful integration of functional groups for drug delivery applications, validating the synthesis of the NPs. Additionally, encapsulation efficiency results indicated a high level of quercetin incorporation into the NPs, supporting their potential as effective drug carriers. Also, the pH-dependent release behavior of NPs suggests that the solubility and/or dissolution rate of Quercetin is reduced in a more alkaline environment. The data indicates that higher drug release at acidic pH conditions, which mimic the tumor microenvironment, leads to enhanced cytotoxicity against cancer cells. The cytotoxicity assay demonstrated a significant decrease in viability for A2780 and AGS cancer cells compared to normal HDF cells, indicating the selective targeting of cancer cells by the NPs. IC50 values highlighted the differential response between cancerous and normal cell lines, suggesting promising prospects for future therapeutic applications. The Annexin V-FITC/PI assay and AO/PI staining provided compelling evidence of the NPs' ability to induce apoptosis in cancer cells in a concentration-dependent manner, further establishing their potential as a therapeutic approach for cancer treatment.

Furthermore, gene expression assays revealed modulation of key genes related to apoptosis, inflammation, and oxidative stress in cancer cells following treatment with the NPs, indicating their potential to influence multiple pathways involved in cancer progression. In addition, the antioxidant capacity assay demonstrated the potent antioxidant properties of the NPs, which effectively neutralized free radicals in a concentration-dependent manner comparable to the performance of the glutathione control. Overall, the comprehensive characterization and evaluation of NCC/CTAB/FA/Quercetin NPs suggest their potential as effective targeted DDSs with promising implications for cancer therapy. These findings lay the groundwork for further exploration of these NPs as potential therapeutic agents in oncology.

Several studies have demonstrated that loading Quercetin onto NPs significantly enhances its cytotoxicity against various cancer cell lines. For example, in an experiment conducted by *Ferreira* and colleagues (2023), chitosan/sulfonyl-ether-β-cyclodextrin (SBE-β-CD)-conjugated delivery systems were investigated to enhance Quercetin's solubility and bioavailability in cervical cancer cells. The research found that formulations with high molecular weight chitosan, SBE-β-CD, and Quercetin produced NPs measuring 272.07 nm, a PDI of 0.287, a zeta potential of + 38.0 mV, and an encapsulation efficiency of around 99.9%. In vitro release studies of 5 kDa chitosan formulations showed 9.6% and 57.53% quercetin release rates at pH 7.4 and 5.8, respectively. The IC50 value on HeLa cells for the HMW chitosan/SBE-β-CD/quercetin delivery system was 43.55 µM, indicating a significant improvement in quercetin bioavailability and cytotoxic effect [42]. In a study by *Keshavarz et al.* (2022), quercetin-loaded nanoliposomes have been shown to increase the cytotoxicity of Quercetin against SW48 colorectal cancer cells. These nanoliposomes reduced the viability of SW48 cells by more than 80% at a concentration of 50 µg/mL, with an IC50 of 10.65 µg/mL, which is more effective than free Quercetin (IC_{50}: 18.74 µg/mL). Additionally, quercetin-loaded nanoliposomes doubled the apoptosis rate compared to free Quercetin [43]. In another work, *Niazvand* and her colleagues (2019) assessed the toxic effects of Quercetin encapsulated in solid lipid NPs (SLNs) on MCF-7 human breast cancer cells. MCF-7 and non-tumorigenic MCF-10 A cells were treated with 25 µmol/mL of Quercetin or quercetin-SLNs for 48 h. Quercetin-SLNs exhibited a particle size of 85.5 nm, a zeta potential of -22.5 mV, and an encapsulation efficiency of 97.6%. They showed sustained release and significantly inhibited MCF-7 cell growth with a lower IC_{50} than free Quercetin. Treatment with quercetin-SLNs reduced cell viability and proliferation while increasing ROS and malondialdehyde (MDA) levels and decreasing antioxidant enzyme activity. Quercetin-SLNs also lowered Bcl-2 expression and increased Bax expression, promoting apoptosis and necrosis in cancer cells. In contrast, neither form affected MCF-10 A cells. The results suggest that SLNs enhance the cytotoxic effects of Quercetin against breast cancer cells [44]. The study conducted by *Karthick et al.* (2019) explored the apoptotic effects of Quercetin extracted from Allium cepa, which was encapsulated in biodegradable poly (lactic-co-glycolic acid) (PLGA) microspheres, on MCF-7. The PLGA microspheres had an average diameter of 100 µm and achieved an encapsulation efficiency of 74 ± 1.2%. Cytotoxicity assessments and flow cytometry revealed that quercetin-PLGA microspheres (PLGAq) significantly inhibited cell growth at higher dosages (1.5 µg and 3.0 µg) by triggering apoptosis. These results indicate that PLGAq microspheres may be a promising therapeutic strategy in breast cancer treatment [45]. *Baksi et al.*

(2018) focused on developing quercetin-loaded chitosan NPs (quercetin-CS NPs) that demonstrated enhanced encapsulation efficiency (79.78%) and sustained release properties. The tiny NPs (< 200 nm) released 67.28% of Quercetin over 12 h at pH 7.4. In vitro, cytotoxicity assays indicated a significantly lower IC_{50} for quercetin-CS NPs than free Quercetin. In vivo studies showed that intravenous treatment of quercetin-CS NPs in tumor xenograft mice reduced tumor volume more effectively than controls, with an increase in serum SOD enzyme levels in the treated group. Overall, the study highlights the successful encapsulation of Quercetin in chitosan NPs for potential cancer therapy [46]. *Ren* and colleagues (2017) investigated using gold-quercetin encapsulated in poly (DL-lactide-co-glycolide) NPs to treat liver cancer. The research revealed that quercetin NPs effectively inhibited the proliferation, migration, and colony formation of liver cancer cells, significantly promoting apoptosis. They found that the NPs facilitated the activation of caspase-9 and caspase-3 and the release of cytochrome c, which are crucial for the apoptosis process. Additionally, they inhibited telomerase reverse transcriptase (hTERT) by reducing the expression of AP-2β and its binding to the hTERT promoter. They also suppressed cyclooxygenase-2 (COX-2) by inhibiting NF-κB activity. Furthermore, quercetin NPs were found to inactivate the Akt/ERK1/2 signaling pathways [47]. In another research, *Sharkar et al.* (2016) developed FA-tagged quercetin-loaded mesoporous silica NPs (MSN-FA-Quercetin) and characterized them using DLS, SEM, TEM, and FTIR. They evaluated cell viability, drug uptake, apoptosis, and other factors in breast adenocarcinoma cells through various assays. The results showed that MSN-FA-Quercetin achieved higher cellular uptake and improved drug bioavailability in MDA MB231 cells, which over-express folate receptors, compared to MCF 7 cells. The NPs induced cell cycle arrest and apoptosis by regulating the Akt and Bax signaling pathways while exhibiting anti-migratory effects. Overall, MSN-FA-Quercetin serves as a targeted delivery system that enhances the bioavailability of Quercetin in breast cancer therapy [48]. *Zhao et al.*. (2016) investigated the therapeutic potential of quercetin-loaded nanomicelles (M-quercetin) for prostate cancer. The study found that M-quercetin could encapsulate Quercetin effectively, increasing its water solubility by 450-fold. In vitro, M-quercetin demonstrated a significantly lower IC50 (20.2 μM) compared to free Quercetin (> 200 μM), leading to better inhibition of cell proliferation and induction of apoptosis in PC-3 cells. In a PC-3 xenograft mouse model, M-quercetin reduced tumor proliferation by 52.03% compared to controls, likely due to enhanced accumulation at the tumor site via the EPR effect. The findings suggest that this nano-micelle-based delivery system is a promising therapeutic strategy for prostate cancer treatment [49].

As mentioned earlier, Quercetin is recognized for its antioxidant properties, which are enhanced when delivered through DDSs. Research has shown that quercetin-loaded chitosan NPs significantly increase oxidative stress markers, such as 8-oxo-dG, cleaved caspase-3, and Bax in SH-SY5Y neuroblastoma cells [50]. This increase leads to DNA damage and apoptosis. In addition, quercetin NPs induce cell cycle arrest at the G1 phase, activate apoptotic pathways involving caspase-3 and cytochrome c release, and promote autophagy through the LC3/ERK/Caspase-3 pathway [51–53]. Furthermore, the evidence demonstrated that Quercetin induces a reversible arrest in the G2/M phase of human promonocytic U937 cells. This effect is associated with significant alterations in cyclins B, D, and E levels. Cyclins D and E downregulation occur through transcriptional suppression rather than affecting protein stability [54]. Quercetin NPs also inhibit critical signaling pathways essential for cancer cell survival, including PI3K/AKT/PKB [55], NF-κB/COX-2 [47], and Wnt/β-catenin [56]. Although specific studies on AGS and ovarian cancer cell lines are limited, the enhanced cytotoxicity and apoptosis induction observed in other cancer models suggest potential therapeutic benefits for these cell types. This is especially promising when Quercetin is combined with other treatments to inhibit metastasis and tumor progression.

Our study highlights the potential of NCC/CTAB/FA/Quercetin NPs as a targeted drug delivery system for cancer therapy. The cytotoxic effects on AGS and A2780 cell lines and their antioxidant properties and apoptosis induction suggest their therapeutic potential.

This study, despite its promising results, has several limitations. First, focusing on only two cancer cell lines (AGS and A2780) may not adequately represent the diversity of cancer types. Therefore, future research should include a broader range of cancer cell lines to enhance the generalizability of the findings. Second, the in vitro nature of the experiments restricts the applicability of the results to in vivo settings; thus, subsequent studies should validate these findings using animal models or clinical trials to assess the therapeutic potential of NCC/CTAB/FA/Quercetin NPs in real biological contexts. Third, while characterization techniques provided valuable insights, they did not fully account for interactions with biological systems that could significantly influence drug delivery and efficacy. Investigating these interactions in greater depth is crucial for understanding the behavior of nanoparticles in biological environments. Fourth, the study did not evaluate the NPs' long-term stability or potential toxicity, both of which are critical factors for their clinical application. Comprehensive assessments of stability under physiological conditions

and potential cytotoxic effects over extended periods are essential for future investigations. Fifth, the analysis of gene expression changes was confined to a select few markers (caspase 8, TNF, SOD, and NF-κB), which may overlook other significant pathways involved in apoptosis and inflammation. Future studies should expand the range of biomarkers analyzed to provide a more comprehensive understanding of the molecular mechanisms at play.

Some recommendations can be proposed to enhance the therapeutic potential of Quercetin-conjugated nanoparticles. Including a broader range of cancer cell lines representing different stages and types will help evaluate efficacy and safety. In vivo experiments are necessary to confirm in vitro findings, focusing on pharmacokinetics, biodistribution, and overall efficacy in animal models. Exploring interactions between nanoparticles and biological components, such as proteins and membranes, will provide insights into drug delivery mechanisms. Investigating long-term nanoparticle stability and assessing potential toxicity with extended exposure studies is vital. Utilizing high-throughput techniques to analyze gene expression changes will deepen the understanding of therapeutic pathways. Addressing these aspects can advance the knowledge and application of Quercetin-conjugated nanoparticles in cancer therapy, ultimately improving patient outcomes.

Conclusion

This study highlights the promising potential of NCC/CTAB/FA/Quercetin NPs as a targeted DDS that significantly enhances the cytotoxicity and antioxidant properties of Quercetin against AGS and A2780 cancer cell lines. The findings align with existing research indicating that such delivery systems can substantially improve Quercetin's solubility, bioavailability, and therapeutic efficacy across various cancer models. The data demonstrate that these NPs facilitate selective targeting and apoptosis of cancer cells and modulate critical pathways associated with oxidative stress and inflammation. Notably, the observed dose-dependent induction of apoptosis, alongside the modulation of gene expression related to inflammatory responses, underscores the therapeutic potential of these NPs in cancer treatment. Given the encouraging results from our study and supporting literature, further investigations into the application of NCC/CTAB/FA/Quercetin NPs as therapeutic agents are warranted. This could lead to the development of more effective cancer treatments with minimized side effects, enhancing patient outcomes in clinical settings.

Author contributions

Mozhgan Soltani, Negar Ahmadzadeh, Hasti Nasiraei Haghighi, Niloufar Khatamian, Masoud Homayouni Tabrizi: Investigation, Methodology and Writing-Original draft. Mozhgan Soltani and Masoud Homayouni Tabrizi: Supervision, Data curation, Conceptualization Software, Validation, and Writing Reviewing.

Funding

This research was performed at personal expense.

Data availability

The datasets used and/or analyzed during the current study are available from the corresponding author upon reasonable request.

Declarations

Ethics approval and consent to participate

All institutional and national guidelines for the care and use of laboratory animals were followed.

Consent for publication

Not applicable.

Competing interests

The authors declare no competing interests.

Received: 1 December 2024 / Accepted: 28 March 2025
Published online: 16 April 2025

References

1. Wang Y, Chen Y, Zhang J, Yang Y, Fleishman JS, Wang Y, et al. Cuproptosis: A novel therapeutic target for overcoming cancer drug resistance. Drug Resist Updates. 2024;72:101018.
2. Patel NR, Pattni BS, Abouzeid AH, Torchilin VP. Nanopreparations to overcome multidrug resistance in cancer. Adv Drug Deliv Rev. 2013;65(13–14):1748–62.
3. Liu Y, Li Q, Zhou L, Xie N, Nice EC, Zhang H, et al. Cancer drug resistance: redox resetting renders a way. Oncotarget. 2016;7(27):42740.
4. Mansoori B, Mohammadi A, Davudian S, Shirjang S, Baradaran B. The different mechanisms of cancer drug resistance: a brief review. Adv Pharm Bull. 2017;7(3):339.
5. Wang X, Zhang H, Chen X. Drug resistance and combating drug resistance in cancer. Cancer Drug Resist. 2019;2(2):141.
6. Man N, Jun Y. Two mutations in TP53 promotes migration, invasion, and proliferation of human ovarian cancer A2780 cells. Russian J Genet. 2020;56:863–8.
7. Yue W, Ma J, Xiao Y, Wang P, Gu X, Xie B, et al. The apoptotic resistance of BRCA1-deficient ovarian cancer cells is mediated by cAMP. Front Cell Dev Biology. 2022;10:889656.
8. Zhao J, Tan W, Zhang L, Liu J, Shangguan M, Chen J, et al. FGFR3 phosphorylates EGFR to promote cisplatin-resistance in ovarian cancer. Biochem Pharmacol. 2021;190:114536.
9. Zhang L, Ma T, Brozick J, Babalola K, Budiu R, Tseng G, et al. Effects of Kras activation and Pten deletion alone or in combination on MUC1 biology and epithelial-to-mesenchymal transition in ovarian cancer. Oncogene. 2016;35(38):5010–20.
10. Seidlitz T, Merker SR, Rothe A, Zakrzewski F, von Neubeck C, Grützmann K, et al. Human gastric cancer modelling using organoids. Gut. 2019;68(2):207–17.
11. Reddy KTK, Reddy AS. Recent breakthroughs in drug delivery systems for targeted cancer therapy: an overview. Cell Mol Biomedical Rep. 2025;5(1):13–27.
12. Shrestha S, Shrestha A, Kim J, Thapa RK, Kim JO. Recent advances in albumin nanoparticle-based cancer therapies. J Pharm Invest. 2025;55(1):1–14.
13. Hazafa A, Rehman K-U-, Jahan N, Jabeen Z. The role of polyphenol (flavonoids) compounds in the treatment of cancer cells. Nutr Cancer. 2020;72(3):386–97.
14. Azeem M, Hanif M, Mahmood K, Ameer N, Chughtai FRS, Abid U. An insight into anticancer, antioxidant, antimicrobial, antidiabetic and anti-inflammatory effects of Quercetin: A review. Polym Bull. 2023;80(1):241–62.
15. Chaichian S, Nikfar B, Bidgoli SA, Moazzami B. The role of Quercetin for the treatment of endometriosis and endometrial cancer: A comprehensive review. Curr Med Chem. 2025;32(1):74–86.
16. Yildirim M, Kilic A, Cimentepe M, Necip A, Turedi S. Synthesis of bioactive quercetin-boronate esters as a novel biological agent: enzyme Inhibition,

anti-microbial properties, computational insights and anticancer activity. J Mol Struct. 2025;1321:140216.
17. Biswas P, Dey D, Biswas PK, Rahaman TI, Saha S, Parvez A, et al. A comprehensive analysis and anticancer activities of Quercetin in ROS-mediated cancer and cancer stem cells. Int J Mol Sci. 2022;23(19):11746.
18. Carrillo-Martinez EJ, Flores-Hernández FY, Salazar-Montes AM, Nario-Chaidez HF, Hernández-Ortega LD. Quercetin, a flavonoid with great Pharmacological capacity. Molecules. 2024;29(5):1000.
19. Gibellini L, Pinti M, Nasi M, De Biasi S, Roat E, Bertoncelli L, et al. Interfering with ROS metabolism in cancer cells: the potential role of Quercetin. Cancers. 2010;2(2):1288–311.
20. Liao Y, Xie X, Zhang C, Zhong H, Shan L, Yu P, et al. Quercetin exerts antitumor immune mechanism by regulating IL-6/JAK2/STAT3 signaling pathway to deplete Treg cells. Toxicon. 2024;243:107747.
21. Wang W, Sun C, Mao L, Ma P, Liu F, Yang J, et al. The biological activities, chemical stability, metabolism and delivery systems of Quercetin: A review. Trends Food Sci Technol. 2016;56:21–38.
22. Kamal R, Singh TG, Bhatia R, Awasthi A. Formulation and evaluation of Mesalamine-Quercetin loaded Self-Nano emulsifying drug delivery systems (SNEDDS) for the management of colon cancer. BioNanoScience. 2025;15(1):1–15.
23. Dang Y, Guan J. Nanoparticle-based drug delivery systems for cancer therapy. Smart Mater Med. 2020;1:10–9.
24. Khan MI, Hossain MI, Hossain MK, Rubel M, Hossain K, Mahfuz A, et al. Recent progress in nanostructured smart drug delivery systems for cancer therapy: a review. ACS Appl Bio Mater. 2022;5(3):971–1012.
25. Jain V, Jain S, Mahajan S. Nanomedicines based drug delivery systems for anticancer targeting and treatment. Curr Drug Deliv. 2015;12(2):177–91.
26. Soltani M, Farhadi A, Rajabi S, Homayouni-Tabrizi M, Hussein FS, Mohammadian N. Folic acid-modified nanocrystalline cellulose for enhanced delivery and anticancer effects of Crocin. Sci Rep. 2024;14(1):13985.
27. Meng L-Y, Wang B, Ma M-G, Zhu J-F. Cellulose-based nanocarriers as platforms for cancer therapy. Curr Pharm Design. 2017;23(35):5292–300.
28. Jackson JK, Letchford K, Wasserman BZ, Ye L, Hamad WY, Burt HM. The use of nanocrystalline cellulose for the binding and controlled release of drugs. Int J Nanomed. 2011;6:321–30.
29. Lugoloobi I, Maniriho H, Jia L, Namulinda T, Shi X, Zhao Y. Cellulose nanocrystals in cancer diagnostics and treatment. J Controlled Release. 2021;336:207–32.
30. Putro JN, Ismadji S, Gunarto C, Yuliana M, Santoso SP, Soetaredjo FE, et al. The effect of surfactants modification on nanocrystalline cellulose for Paclitaxel loading and release study. J Mol Liq. 2019;282:407–14.
31. Teow Y, Valiyaveettil S. Active targeting of cancer cells using folic acid-conjugated platinum nanoparticles. Nanoscale. 2010;2(12):2607–13.
32. Namvar F, Azizi S, Rahman HS, Mohamad R, Rasedee A, Soltani M, et al. Green synthesis, characterization, and anticancer activity of hyaluronan/zinc oxide nanocomposite. OncoTargets Therapy. 2016;9:4549–59.
33. Bray F, Laversanne M, Sung H, Ferlay J, Siegel RL, Soerjomataram I, et al. Global cancer statistics 2022: GLOBOCAN estimates of incidence and mortality worldwide for 36 cancers in 185 countries. Cancer J Clin. 2024;74(3):229–63.
34. Ilic M, Ilic I. Cancer of colon, rectum and anus: the rising burden of disease worldwide from 1990 to 2019. J Public Health. 2024;46(1):20–9.
35. Nikolaou M, Pavlopoulou A, Georgakilas AG, Kyrodimos E. The challenge of drug resistance in cancer treatment: a current overview. Clin Exp Metastasis. 2018;35:309–18.
36. Khan SU, Fatima K, Aisha S, Malik F. Unveiling the mechanisms and challenges of cancer drug resistance. Cell Communication Signal. 2024;22(1):109.
37. Pérez-Herrero E, Fernández-Medarde A. Advanced targeted therapies in cancer: drug nanocarriers, the future of chemotherapy. Eur J Pharm Biopharm. 2015;93:52–79.
38. Cai Z-M, Li Z-Z, Zhong N-N, Cao L-M, Xiao Y, Li J-Q, et al. Revolutionizing lymph node metastasis imaging: the role of drug delivery systems and future perspectives. J Nanobiotechnol. 2024;22(1):135.
39. Kapoor DU, Sharma JB, Gandhi SM, Prajapati BG, Thanawuth K, Limmatvapirat S, et al. AI-driven design and optimization of nanoparticle-based drug delivery systems. Sci Eng Health Stud. 2024;18:24010003.
40. Shao X, Zhao X, Wang B, Fan J, Wang J, An H. Tumor microenvironment targeted nano-drug delivery systems for multidrug resistant tumor therapy. Theranostics. 2025;15(5):1689.
41. Long J, Liang X, Ao Z, Tang X, Li C, Yan K, et al. Stimulus-responsive drug delivery nanoplatforms for inflammatory bowel disease therapy. Acta Biomater. 2024;188(10):27–47.
42. Ferreira M, Gomes D, Neto M, Passarinha LA, Costa D, Sousa Â. Development and characterization of quercetin-loaded delivery systems for increasing its bioavailability in cervical cancer cells. Pharmaceutics. 2023;15(3):936.
43. Keshavarz F, Dorfaki M, Bardania H, Khosravani F, Nazari P, Ghalamfarsa G. Quercetin-loaded liposomes effectively induced apoptosis and decreased the epidermal growth factor receptor expression in colorectal cancer cells: an in vitro study. Iran J Med Sci. 2023;48(3):321.
44. Niazvand F, Orazizadeh M, Khorsandi L, Abbaspour M, Mansouri E, Khodadadi A. Effects of quercetin-loaded nanoparticles on MCF-7 human breast cancer cells. Medicina. 2019;55(4):114.
45. Karthick V, Panda S, Kumar VG, Kumar D, Shrestha LK, Ariga K, et al. Quercetin loaded PLGA microspheres induce apoptosis in breast cancer cells. Appl Surf Sci. 2019;487:211–7.
46. Baksi R, Singh DP, Borse SP, Rana R, Sharma V, Nivsarkar M. In vitro and in vivo anticancer efficacy potential of Quercetin loaded polymeric nanoparticles. Biomed Pharmacother. 2018;106:1513–26.
47. Ren K-W, Li Y-H, Wu G, Ren J-Z, Lu H-B, Li Z-M, et al. Quercetin nanoparticles display antitumor activity via proliferation Inhibition and apoptosis induction in liver cancer cells. Int J Oncol. 2017;50(4):1299–311.
48. Sarkar A, Ghosh S, Chowdhury S, Pandey B, Sil PC. Targeted delivery of Quercetin loaded mesoporous silica nanoparticles to the breast cancer cells. Biochim Et Biophys Acta (BBA)-General Subj. 2016;1860(10):2065–75.
49. Zhao J, Liu J, Wei T, Ma X, Cheng Q, Huo S, et al. Quercetin-loaded nanomicelles to circumvent human castration-resistant prostate cancer in vitro and in vivo. Nanoscale. 2016;8(9):5126–38.
50. Dogan M. Assessment of mechanism involved in the apoptotic and anticancer activity of Quercetin and Quercetin-loaded Chitosan nanoparticles. Med Oncol. 2022;39(11):176.
51. Choi J-A, Kim J-Y, Lee J-Y, Kang C-M, Kwon H-J, Yoo Y-D, et al. Induction of cell cycle arrest and apoptosis in human breast cancer cells by Quercetin. Int J Oncol. 2001;19(4):837–44.
52. Bishayee K, Ghosh S, Mukherjee A, Sadhukhan R, Mondal J, Khuda-Bukhsh A. Quercetin induces cytochrome-c release and ROS accumulation to promote apoptosis and arrest the cell cycle in G2/M, in cervical carcinoma: signal cascade and drug-DNA interaction. Cell Prolif. 2013;46(2):153–63.
53. Zhou J, Li L, Fang L, Xie H, Yao W, Zhou X, et al. Quercetin reduces Cyclin D1 activity and induces G1 phase arrest in HepG2 cells. Oncol Lett. 2016;12(1):516–22.
54. Lee T-J, Kim OH, Kim YH, Lim JH, Kim S, Park J-W, et al. Quercetin arrests G2/M phase and induces caspase-dependent cell death in U937 cells. Cancer Lett. 2006;240(2):234–42.
55. Gulati N, Laudet B, Zohrabian VM, Murali R, Jhanwar-Uniyal M. The antiproliferative effect of Quercetin in cancer cells is mediated via Inhibition of the PI3K-Akt/PKB pathway. Anticancer Res. 2006;26(2A):1177–81.
56. Kumar D, Sharma PK, Quercetin. A comprehensive review. Curr Nutr Food Sci. 2024;20(2):143–66.

Publisher's note